

Paper:

# Evaluating Functional Connectivity in Alcoholics Based on Maximal Weight Matching

Guohun Zhu<sup>\*,\*\*\*</sup>, Yan Li<sup>\*,\*\*\*</sup>, and Peng (Paul) Wen<sup>\*\*,\*\*</sup>

<sup>\*</sup>Department of Mathematics and Computing, University of Southern Queensland

<sup>\*\*</sup>Faculty of Engineering and Surveying, University of Southern Queensland

<sup>\*\*\*</sup>Centre for Systems Biology, University of Southern Queensland

USQ Toowoomba Campus, West Street, Toowoomba, QLD 4350, Australia

E-mail: {Guohun.Zhu, Yan.Li, Peng.Wen}@usq.edu.au

[Received March 2, 2011; accepted September 29, 2011]

**EEG-based applications have faced the challenge of multi-modal integrated analysis problems. In this paper, a greedy maximal weight matching approach is used to measure the functional connectivity in alcoholics datasets with EEG and EOG signals. The major discovery is that the processing of the repeated and unrepeated stimuli in the  $\gamma$  band in control drinkers is significantly more different than that in alcoholic subjects. However, the EOGs are always stable in the case of visual tasks, except for a weakly wave when subjects make an error response to the stimuli.**

**Keywords:** EEG, greedy maximal weight matching, synchronization, repeated and unrepeated stimuli

## 1. Introduction

In recent years, electroencephalograms (EEGs) have been widely used to evaluate the dysfunction of alcoholic persons' brain. Researchers mainly focused on four frequency bands,  $\theta$  (4–8 Hz),  $\alpha$  (8–12.5 Hz),  $\beta$  (12.5–28.5 Hz) and  $\gamma$  (28.5–45 Hz). In the  $\theta$  band, heavy drinkers have better synchronization than control subjects with 62-tin electrodes [1]. In the  $\alpha$  band, alcoholics have lower activity in the left anterior cortex than in the right anterior cortex [2]. Michael et al. also found that the  $\alpha$  coherence increases at the central region [3]. Winterer et al. [4] found that the posterior coherence of alcoholics are significantly increased both in  $\alpha$  band and  $\beta$  band. Moreover, heavy drinkers have higher synchronization in  $\gamma$  band [1]. However, an optimal brain function has a high synchronization which is different from the increase coherence of alcoholics [5]. In fact, increasing coherence on alcoholics is also in contrast to the study on a public 61-channels EEG alcoholics dataset with two electrooculogram (EOG) signals. By event related potential (ERP) technique, it was found the right hemisphere of alcoholics is depressed unlike that of control drinkers [6]. Moreover, using a synchrony visualization method, Sakkalis [7] found that alcoholics had impaired synchronization in  $\alpha$  band and low  $\beta$  synchroniza-

tion than control drinkers. Therefore, increase or decrease synchronization was result from inconsistency in alcoholic databases. Because there is no efficient way to study functional connectivity of the human brain using multi-channel and multi-modal data. In fact, supporting multi-modal data integration and fusion is one of challenges in EEG-based applications, especially with wireless sensor networks [8] and ubiquitous networks [9]. This paper will use a graph theory to study this challenge and investigate the functional connectivity using both EEG and EOG data.

Graph theoretical methods have been employed to study EEGs for about a decade. A popular approach is based on a small-world network [10]. The functional connectivity of the human brain has been proved to be a small-world network by some researchers [11, 12]. The approach is to map a synchronization matrix into a binary graph  $G$ , in which nodes of  $G$  are mapped from electrodes and the weight of each edge of  $G$  is the synchronization value between two electrode pairs. However, the properties of a small-world network only describe the clustering and the small-world effect in the whole graph. It can not be used to analyze the functional connectivity between pair-wise nodes.

The aim of this study is to investigate the visual stimuli of the different brain regions of alcoholics with that of the different brain regions of control drinkers, with maximal weight matching on a multi-modal datasets. The data set in this study includes 11,035 EEG recordings where 7,014 trials are alcoholics, while the rest are control drinkers. To study the functional connectivity between five regions of the cortex, the raw data were processed in four steps. Firstly, a band-pass filter is used to extract the four bands from the raw data. Secondly, the autocorrelation of a short time series is calculated with high dimensional embedding vector. The coupled Hénon system is used as a reference to verify the approach. Then the synchronization matrix of each recording is mapped into a weighted graph  $G$  and the greedy maximal weight matching  $M$  of  $G$  is obtained for alcoholics and control drinkers, respectively. The electrode pairs of  $M$  are encoded according to the electrode pairs directions and regions. Lastly, the average of the maximal weight matching both for alco-

holics and control drinkers is statistically analyzed separately. The maximal weight matching on 8, 19, and 61 channels are computed and are used to evaluate which directions and regions of synchronizations are enhanced or decreased when different stimuli are applied.

## 2. Methodology

### 2.1. The Alcoholic Data Set and the Optimal Channels

The experimental data were taken from a public EEG database. The experiments were performed on 122 subjects. Each subjects went through 120 trials and with three types of stimuli [6]: *S1* (one stimulus presentation), *S2M* (one picture stimulus twice) and *S2N* (the second test picture is different from the first time). In the case of *S2M* and *S2N*, the task was that the subjects should decide whether the second picture was the same as the first stimulus [6]. If the decision was incorrect, the data was marked as *S2Merr*, *S2Nerr*, respectively. There were three datasets on this database: TRAIN, TEST and FULL. It should be noted that the FULL dataset included the previous two data sets, but it had a different number of alcoholics and control drinker trials. It also contained a few all-zero recordings, which should be careful for processing these padding zeros. This paper studied the FULL dataset in four frequency bands:  $\theta$  band (4–8.5 Hz),  $\alpha$  band (8.5–12 Hz),  $\beta$  band (12–28.5 Hz) and  $\gamma$  band (28.5–45 Hz).

Because the EEG data sets were collected with 63 electrode caps, it is not necessary to analyze all channels in general case. Palaniappan [13] used a genetic algorithm to select the eight optimal channels (Pz, P7, O2, FPz, TP7, P6, C1, FCz) to classify the alcoholics and control drinkers on the basis of dataset TRAIN and TEST in  $\gamma$  band. Some studies [2, 14] used the channels: FP1, FP2, F7, F3, Fz, F4, F8, T7, C3, Cz, C4, T8, P7, P3, Pz, P4, P8, O1 and O2 for the specified measurement. This study uses the maximal weight matching method to evaluate the performance of these optimal channels.

### 2.2. Filtering and Autocorrelation

This section discusses two key processing techniques for short time series with each signal having 256 points being recorded for 1 s. One key process is to filter out the data from the lower band and another is to extract the attractor from the short time-series EEGs.

Filtering is a necessary preprocessing step to separate the band from the raw EEG data. For example, to extract the  $\gamma$  band from the raw data, the digital Butterworth filter was used in [15], and a band-pass filter construct with low-pass filter and high-pass filter was used in [13]. The filtering results greatly affect the process of EEG, especially on the low frequency band.

Figure 1 illustrates a case of the band-pass filter on the lower frequency signals. To obtain  $\theta$  (4–8.5 Hz) from one channel of *co2a000364* subject in 0 trial, the *F3*  $\theta$  waves

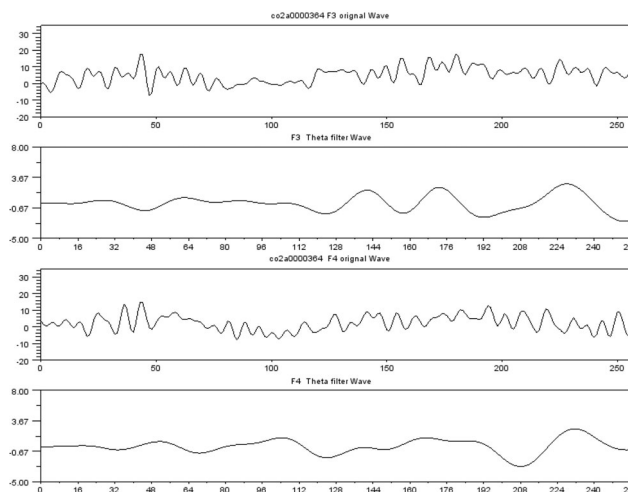


Fig. 1. An example of the filter effect the data.

and *F4*  $\theta$  waves, shown in Fig. 1, were employed after it was filtered using the following SCILAB IIR filtering method.

$$[lisys] = iir(4, 'bp', 'cheb1', [0.014, 0.031], [0.01, 0.06]);$$

It is easy to observe that both filtered signals are smoothed from zero to five points, which increase the coherence if these two time series are analyzed. Therefore, the first four points are ignored and only 252 points were used.

EEG signals can be viewed as a nonlinear dynamical system that can be extracted by the attractor in the phase space [16]. To classify single trial EEG time series  $T = [t_1, t_2, \dots, t_N]$ ,  $T$  can be converted to a  $m$ -dimensional embedding vector  $X \in R^m$ .

$$Xi = T[i], T[i + \tau], \dots, T[i + (m - 1)\tau] \quad \dots \quad (1)$$

where  $i = 1, 2, \dots, N_e = N - m\tau$  and  $\tau$  is the time delay. Then, the autocorrelation factor of  $T$  can be obtained from the phase space  $X$  by employing the Theiler method [16]. However, Theiler algorithm is more complex and does not works well on short time series data, so a simple approach is used in this study to obtain the autocorrelation factor  $C_r$ , which is calculated using Eq. (2).

$$C_r = \frac{1}{N_e + 1} \sum_{j=i+w}^{N_e} \sigma(|X_i - X_j|), i \in [1, \dots, N_e] \quad (2)$$

where  $w$  is Theler window,  $\sigma$  is Heavisible function,  $\sigma(x) = 1$  if  $x > 0$ ; otherwise  $\sigma(x) = 0$ . It is noted that Eq. (2) is more efficient than the probability approach in [17], because the probability step is ignored in this equation.

$C_r$  is sensitive to  $w$  and  $m$  in a short time series. Sanz-Arigita [18] illustrated an example to set up the parameters for a smaller data set, where  $m = 6$  and  $w = 6$ . However, according to Takens's idea [19],  $m > 2d$ , where  $d$  is the dimension of the system on the attractor. Therefore,  $d < 3$  when  $m = 6$ , which should not be a real feature of the attractor for the EEG series. In this paper, the param-

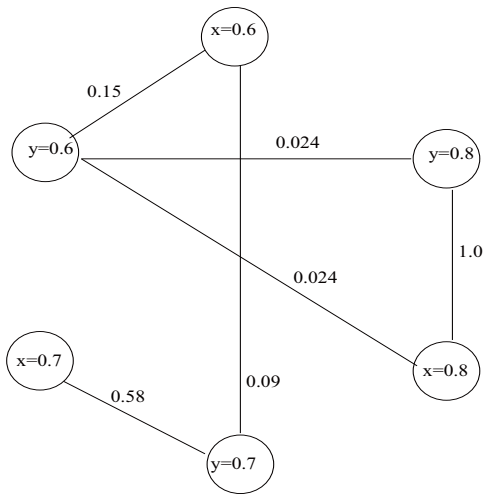


Fig. 2. A graph of the Hénon system ( $B = 0.3$ ).

eters are as follows:  $\tau = 1$ ,  $m = 26$  and  $w = 64$ , which are suitable for extracting the attractor from the 256 EEG points.

### 2.3. Mapping a Synchronization Matrix into a Graph

Synchronization Likelihood (SL) was proposed by Stam [17], and it was used to calculate the distance between two series in the phase space. The synchronization of any two channels  $T_i$  and  $T_j$  is given by

$$\left. \begin{aligned} H_{i,j} &= \sum_{k=1}^m \sigma(C_r(k) - |X_{k,i} - Y_{k,j}|) \\ SL_{i,j} &= \frac{1}{2m} \sum_{k=1}^m H_{i,k} + H_{j,k} \end{aligned} \right\} \dots \dots (3)$$

where  $X_{m,i}$  and  $Y_{m,j}$  are  $m$ -dimensional embedding vector of  $T_i$  and  $T_j$ , respectively.

It is clear that the range of  $SL_{i,j}$  is between 0 and 1. In general, the synchronization matrix is mapped into a binary graph [18]. Because  $SL_{i,j} = SL_{j,i}$ , let  $SL_{i,i} = 0$ ,  $SL$  is a symmetric and can be represented as an adjacency matrix of a graph, where nodes represent channels, and edges are the synchronization value between two channels. Therefore the synchronization matrix is mapped into a weighted graph in this study.

It is noted that Eqs. (2) and (3) are different [17]. To verify these equations, an identical Hénon system is used in this paper, which was also used in [17].

$$\left. \begin{aligned} x_{i+1} &= 1.4 - x_i^2 + 0.3u_i \\ y_{i+1} &= 1.4 - (Cx_i + (1 - C)y_i)y_i + Bv_i, \\ u_{i+1} &= x_i, v_{i+1} = y_i \end{aligned} \right\} \dots (4)$$

where  $x_0$ ,  $y_0$ ,  $u_0$  and  $v_0$  are initialized to random values. Fig. 2 is a graph mapping from the coupled Hénon system with parameters  $B = 0.3$  and  $C = 0.6$  to  $0.8$ , where SL parameters are  $\tau = 1$ ,  $m = 26$ ,  $w = 64$  and  $N = 256$ . For simplification, the weights less than 0.02 are ignored. It is easy to verify that the results are similar with those in [17].

### 2.4. Greedy Maximal Matching on the Regions of the Brain

A matching in graph  $G$  is a subset of pair-wise non-adjacent edges; that is, no two edges share a common vertex. A greedy weight matching  $M$  is the one for which the sum of the weights of the edges of  $M$  is maximal with a greedy method. For example, Fig. 2 has a greedy weight matching  $M = \{x = 0.8, y = 0.8\}, \{x = 0.7, y = 0.7\}, \{x = 0.6, y = 0.6\}$ . The total weight is  $w(M) = 1.73$  and the highest weight edge  $\{x = 0.8, y = 0.8\}$  belongs to  $M$ .

Maximum matching problems are well-known problems in graph theory and are proved to be solved with a complexity of  $O(n^3)$  [20]. Certainly, there exists an optimal algorithm for processing EEGs. For example, the optimal pairing of signal components are separated by comparing with a greedy approach [21]. However, maximum weight matching do not always include the highest weight edges [21]. Therefore, the greedy algorithm is used to ensure that the highest weight edge is always included in the matching. In this paper, the algorithm is greedy and recursive. First, the most weight edge  $e$  is selected from  $G$  into  $M$ , then  $e$  and the two connected nodes are removed from  $G$ , and this procedure is repeated until the number of remaining nodes is less than two. The details of the greedy algorithm is presented in [22].

To measure the effect of the pairwise electrodes, the brain is divided into six regions: Frontal ( $F$ ), Central ( $C$ ), Parietal ( $P$ ), Occipital ( $O$ ), Temporal ( $T$ ) and  $EOG$  regions. The first five regions include the electrodes following the rules in [6]. The  $F$  region consisted of  $FP1, FP2, FPz, AF1, AF2, AF7, AF8, AFz, F1, F2, F3, F4, F5, F6, F7, F8$  and  $Fz$ . The  $C$  region consisted of  $Fc1, Fc2, Fc3, Fc4, Fc5, Fc6, C1, C2, C3, C4, C5$ , and  $C6$ . The  $P$  region consisted of  $Cp1, Cp2, Cp3, Cp4, Cpz, P1, P2, P3, P4$  and  $Pz$ . The  $O$  region consisted of  $Po1, Po2, Po7, Po8, Poz, O1, O2$ , and  $Oz$ . The  $T$  region consisted of  $T7, T8, Tp7, Tp8, Cp5, Cp6, P7$  and  $P8$ . The  $EOG$  region consisted of  $X$  and  $Y$  electrodes. To more precisely evaluate the affect on the left or right hemisphere, three groups are defined: left( $L$ ), right( $R$ ) and join( $J$ ). For example, the matching  $M_1 = \{F3, F7\}$  is encoded  $F.L$  and implies that the pair-wise electrodes belong to left frontal region,  $M_2 = \{P4, P8\}$  is  $P.R$  and implies that the pair-wise electrodes belong to right parietal region,  $M_3 = \{O1, O2\}$  is  $O.J$  and implies that the pair-wise electrodes belong to left and right occipital region.

## 3. Results and Discussions

### 3.1. Verifying the Optimal Channel Numbers Using Greedy Maximal Weight Matching

Three different channel numbers: 8, 19 and 63 are analyzed using the greedy maximal weight matching in  $\gamma$  band, which are shown in Figs. 3–5. Figs. 3 and 5 indicate significant differences between alcoholics and control drinkers. However the differences between alcoholics and control drinkers are smaller, under in the case of the

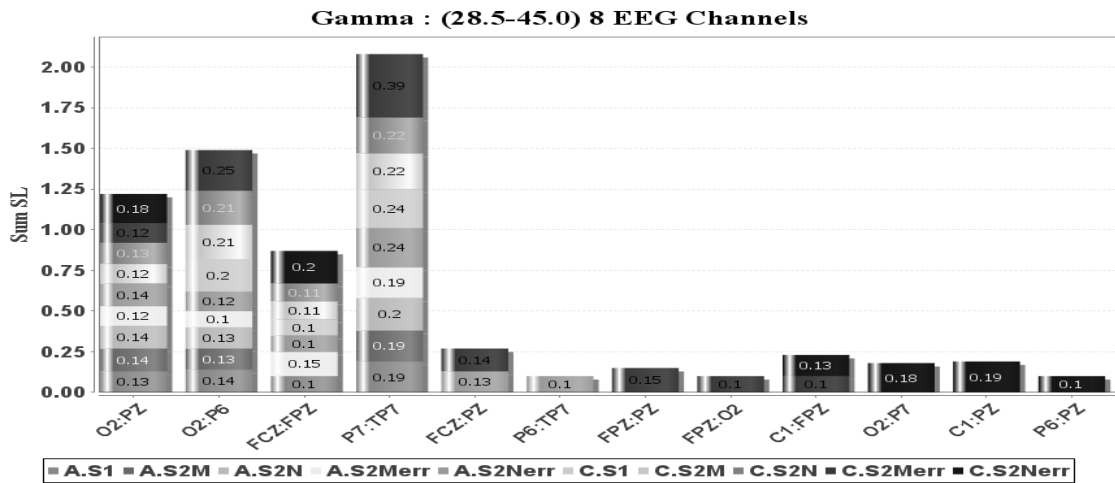


Fig. 3.  $\gamma$  on FULL dataset with 8 channels.

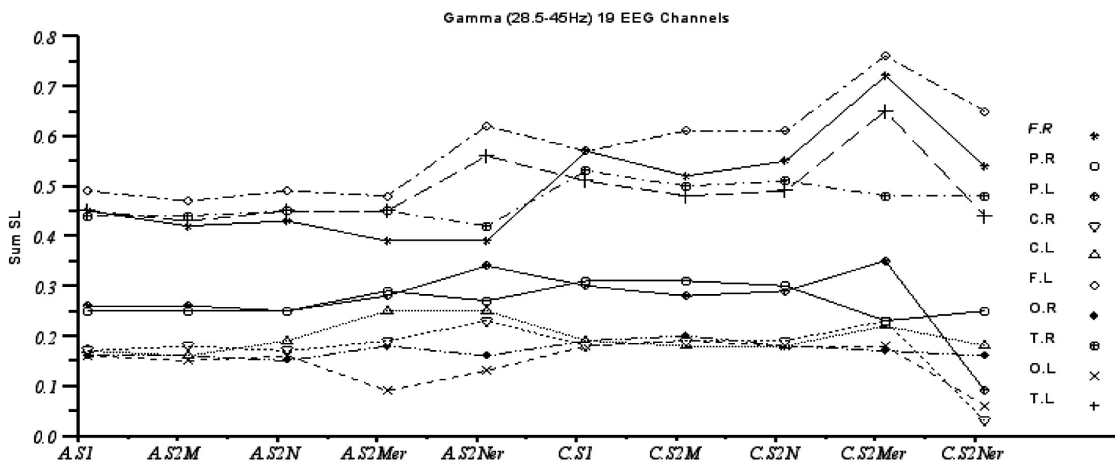


Fig. 4.  $\gamma$  on FULL dataset with 19 channels.

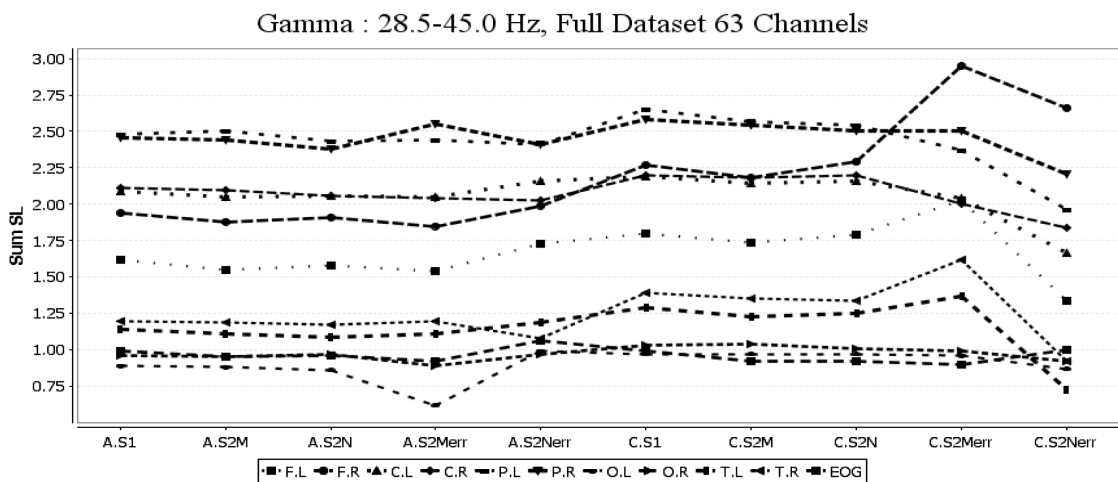


Fig. 5.  $\gamma$  on FULL dataset with 61 EEGs and 2 EOGs.

**Table 1.** Running time for three types of channel numbers.

databases	trials	8 optima channels	19-channel	63-channel
TEST	600	8.5	13.5	25.5
TRAIN	600	8.5	13.6	25.7
FULL	11035	17.31	258.7	761

**Table 2.** Average of 11,035 trials SL on FULL dataset.

a: alcoholics, c: control drinkers.

Stimuli Hz	S1 Obj		S2 Match		S2 Nomatch	
	a	c	a	c	a	c
$\gamma$	0.188	0.200	0.184	0.196	0.182	0.198
$\beta$	0.239	0.251	0.233	0.236	0.240	0.244
$\alpha$	0.265	0.275	0.273	0.275	0.279	0.278
$\theta$	0.308	0.314	0.308	0.307	0.310	0.313

19-channel EEG, as shown in **Fig. 4**. For instance, control drinkers have a higher pair-wise  $\{O2, P6\}$  than alcoholics, in the case of the 8-channel EEGs; the pair-wise  $\{FCz, Pz\}$  is never shown in the  $S2Nerr$  of control drinkers. On the other hand, the control drinkers have a higher SL value in  $F.R$  than alcoholics do, on a 63-channel EEGs and EOGs (**Fig. 5**). However, it is difficult to divide the control drinkers and alcoholics from **Fig. 4** because the values of  $F.L$  and  $F.R$  on  $C.S1$  are lower than  $A.S2Nerr$ . To evaluate the complexity of 8 optimal channels [13], the basic 19-channel [2, 14], and the 63-channel in this study, the running time of the three types of channels are listed in **Table 1**.

### 3.2. The SL of Alcoholism and Controller on Different Stimuli

The results of this study on the average of SL are different from the results in [1]. 77 alcohol subjects and 45 control drinkers of FULL datasets are analyzed by applying three different stimuli. The analysis results of FULL dataset are shown in **Table 2**. In the case of  $\gamma$  band, the average synchronization in alcoholics is less than that in control drinkers, which is consistent with the result in [15], but it is different from the result in [1]. This is because the test data do not include data about the eye and body movements [6]. On the other hand, in the  $\alpha$  band, the alcoholics have a better synchronization than control drinkers do, which agrees with the  $\alpha$  band result in [1].

Further, an interesting discovery is that the left cortex of alcoholics is different from that of control drinkers in the  $\gamma$  band. The results are shown in **Table 3**. The synchronization of the left and right brain of subjects are always increased during  $\beta$ ,  $\alpha$  and  $\theta$  bands. Conversely, the synchronization of the left cortex of alcoholics and control drinkers are stable in  $\gamma$  band in 4.6 and 4.9 respectively, and the synchronization value of the right cortex are decreased from 4.73 to 4.7 in alcoholics but a increase slightly in control drinkers. Therefore, the abnormal synchronization of  $\gamma$  band on the left and right hemisphere implies that the alcoholics process the repeated and unrepeated stimuli different from the control drinkers. The

**Table 3.** Mean and SD of the left and right on FULL dataset.

M: S2M, N: S2N.

B	T	alcohol		controller	
		L	R	L	R
$\gamma$	M	4.6 ± 1.55	4.73 ± 1.59	4.9 ± 1.57	5.11 ± 1.65
	N	4.6 ± 1.59	4.7 ± 1.57	4.9 ± 1.5	5.13 ± 1.66
$\beta$	M	5.85 ± 2.04	6 ± 2.11	5.86 ± 2	6.17 ± 2.13
	N	6 ± 2.08	6.17 ± 2.16	6.06 ± 2.05	6.33 ± 2.1
$\alpha$	M	6.86 ± 2.46	7.11 ± 2.57	6.89 ± 2.38	7.21 ± 2.42
	N	6.96 ± 2.4	7.27 ± 2.51	6.97 ± 2.41	7.29 ± 2.54
$\theta$	M	7.75 ± 2.25	8.01 ± 2.29	7.72 ± 2.22	8 ± 2.36
	N	7.81 ± 2.29	8.07 ± 2.3	7.87 ± 2.2	8.16 ± 2.25

next section will use maximal weight matching to enhance these results on all wave bands.

### 3.3. The Functional Connectivity During Repeated and Unrepeated Stimuli

Although both **Figs. 3** and **5** show a good synchronization of  $\gamma$  band in the parietal region of alcoholic and control drinkers, the  $S2Merr$  and  $S2Nerr$  of alcoholics and control drinkers show significantly different trends. For instance, except  $P.R$ ,  $T.R$  and  $EOG$ , all regions are decreased from  $S2Merr$  to  $S2Nerr$  in control drinkers, but they are stable, only slightly increased in alcoholics. These imply that the functional connectivity are different while repeated and unrepeated stimuli are applied in alcoholics and control drinkers. **Figs. 6–8** demonstrate these results in  $\beta$ ,  $\alpha$  and  $\theta$  wave bands. For example, in **Fig. 6**, for the  $\beta$  band, except  $P.R$ , all areas are decreased from  $S2Merr$  to  $S2Nerr$  in the case of control drinkers,  $P.R$ ,  $C.R$ ,  $F.R$ ,  $F.L$ ,  $T.L$  and  $EOG$  are increased in the case of alcoholics. In contrast, it is noted that the  $\alpha$  band is different from  $\gamma$  and  $\beta$  bands, as shown in **Fig. 7**. Only  $O.L$  and  $F.L$  are decreased from  $S2Merr$  to  $S2Nerr$  in the case of alcoholics, while other regions are increased. However, only half the regions of control drinkers are increased, while the other half is decreased. In **Fig. 8**, all regions of control drinkers are decreased, but  $F.L$  is slightly decreased on alcoholics. Furthermore, the synchronization of the  $\alpha$  band is higher than that of the other bands in the parietal regions, which is consistent with the results in [7]; and the ratio of  $\alpha$  band synchronization in the left to that in the right regions is higher than the synchronization of other bands. The  $P.R$ ,  $C.L$  are larger than  $P.L$ ,  $C.R$  in  $S2Nerr$  for the control drinkers; but are approximately equal in alcoholics. These EEG phenomena imply that there are different processing procedures in different regions of alcoholics and control drinkers with the repeated stimuli and unrepeated stimuli.

There is an interesting finding in this dataset: the  $EOG$  is very stable from **Figs. 5–8**, irrespective of whether on alcoholics or on control drinkers, with only a weak decrease in  $S2Nerr$  in the case of control drinkers. The results imply that the alcoholics are not affected by the EOG signal, because the EOG does not represent the response to visual stimuli.

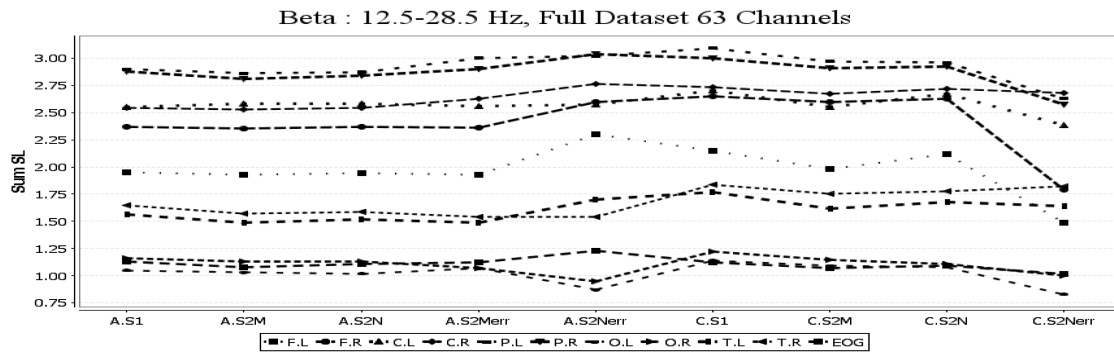


Fig. 6.  $\beta$  on FULL dataset with 61 EEGs and 2 EOGs.

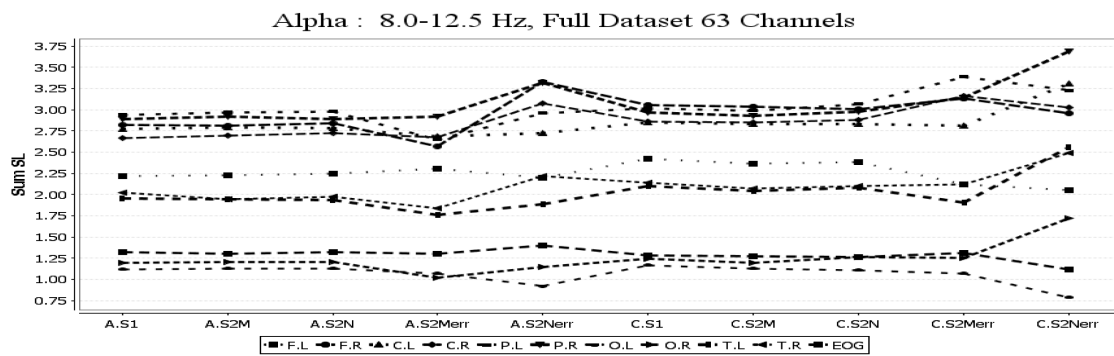


Fig. 7.  $\alpha$  on FULL dataset with 61 EEGs and 2 EOGs.

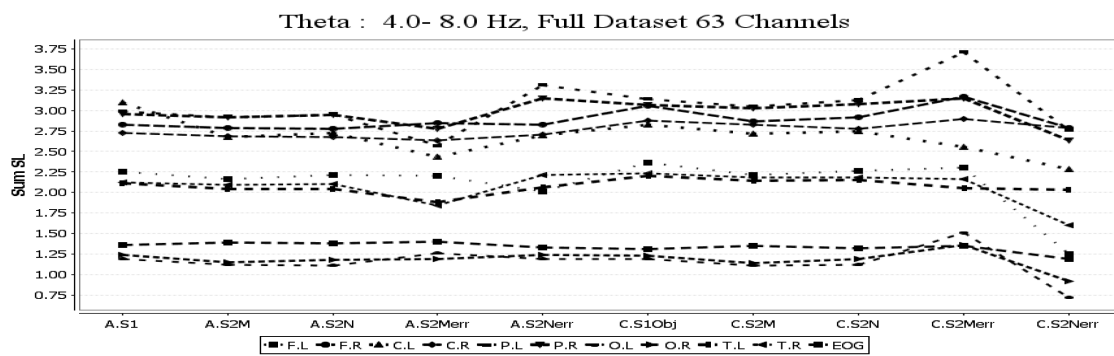


Fig. 8.  $\theta$  on Full dataset with 61 EEGs and 2 EOGs.

#### 4. Conclusions

In this paper, the greedy maximum weight matching analysis on the functional connectivity in human brain is proposed. This is the first time that the functional connectivity between EEG and EOG is investigated. It is also the first time that a classical graph algorithm is used to study the synchronization of EEG phenomena. Compared with the modern small-world graph theories, this approach can classify the repeated and un-repeated stimuli on control drinkers, and can be used as a testbench for the selection of optimal channel numbers. Moreover, this study indicates that the maximal weight matching combined with synchronization can be a useful tool to eval-

uate the abnormal EEG signals. It is also found that the difference functional connectivity for processing repeated stimuli and un-repeated stimuli in the control drinkers are larger than that in the alcoholics. Moreover, it shows that the *EOG* is not sensitive with the alcoholics.

#### Acknowledgements

The authors thank Henri Begleiter at the Neurodynamic Laboratory, State University of New York Health Center, Brooklyn, USA, who recorded the raw EEG data used in this paper.

**References:**

- [1] E. A. de Bruin, S. Bijl, et al., "Abnormal EEG synchronization in heavily drinking students," *Clinical Neurophysiology*, Vol.115, No.9, pp. 2048-2055, 2004.
- [2] E. P. Hayden, R. E. Wiegand, et al., "Patterns of Regional Brain Activity in Alcohol-Dependent Subjects," *Alcoholism: Clinical and Experimental Research*, Vol.30, No.12, pp. 1986-1991, 2006.
- [3] A. Michael et al., "Interhemispheric electroencephalographic coherence as a biological marker in alcoholism," *Acta Psychiatrica Scandinavica*, Vol.87, pp. 213-217, 1993.
- [4] G. Winterer et al., "EEG phenotype in alcoholism: increased coherence in the depressive subtype," *Acta Psychiatrica Scandinavica*, Vol.108, pp. 51-60, 2003.
- [5] P. E. Keller, G. Knoblich, et al., "Pianists duet better when they play with themselves: On the possible role of action simulation in synchronization," *Consciousness and Cognition*, Vol.16, No.1, pp. 102-111, 2007.
- [6] X. L. Zhang, H. Begleiter, et al., "Electrophysiological evidence of memory impairment in alcoholic patients," *Biological Psychiatry*, Vol.42, No.12, pp. 1157-1171, 1997.
- [7] V. Sakkalis et al., "Optimal brain network synchrony visualization: Application in an alcoholism paradigm," in *Engineering in Medicine and Biology Society, 2007 (EMBS 2007), 29th Annual Int. Conf. of the IEEE, Lyon*, pp. 4285-4288, October 22, 2007.
- [8] P. Salvador, et al., "Markovian Models for Medical Signals on Wireless Sensor Networks," in *Communications Workshops, 2009, ICC Workshops 2009, IEEE Int. Conf. on*, pp. 1-5, 2009.
- [9] B. Hu, et al., "EEG-Based Cognitive Interfaces for Ubiquitous Applications: Developments and Challenges," *Intelligent Systems, IEEE*, Vol.26, pp. 46-53, 2011.
- [10] D. J. Watts, S. H. Strogatz, "Collective dynamics of 'small-world' networks," *Nature*, Vol.393, pp. 440-442, 1998.
- [11] M. D. Humphries, K. Gurney, et al., "The brainstem reticular formation is a small-world, not scale-free, network," *Proc. of the Royal Society B: Biological Sciences*, Vol.273, No.1585, pp. 503-511, 2006.
- [12] S. Michelyoyannis, E. Pachou, et al., "Using graph theoretical analysis of multi channel EEG to evaluate the neural efficiency hypothesis," *Neuroscience Letters*, Vol.402, No.3, pp. 273-277, 2006.
- [13] R. Palaniappan, P. Raveendran, et al., "VEP optimal channel selection using genetic algorithm for neural network classification of alcoholics," *IEEE Trans. on Neural Networks*, Vol.13, No.2, pp. 486-491, 2002.
- [14] M. Rangaswamy, B. Porjesz, et al., "Resting EEG in offspring of male alcoholics: beta frequencies," *Int. J. of Psychophysiology*, Vol.51, No.3, pp. 239-251, 2004.
- [15] K. Ravi and R. Palaniappan, "Neural network classification of late gamma band electroencephalogram features," *Soft Computing – A Fusion of Foundations, Methodologies and Applications*, Vol.10, No.2, pp. 163-169, 2006.
- [16] J. Theiler, "Spurious dimension from correlation algorithms applied to limited time-series data," *Physical Review A*, Vol.34, No.3, pp. 2427-2432, 1986.
- [17] C. J. Stam and B. W. van Dijk, "Synchronization likelihood: an unbiased measure of generalized synchronization in multivariate data sets," *Physica D: Nonlinear Phenomena*, Vol.163, No.3, pp. 236-251, 2002.
- [18] E. J. Sanz-Arigita et al., "Loss of 'Small-World' Networks in Alzheimer's Disease: Graph Analysis of fMRI Resting-State Functional Connectivity," *PLoS ONE*, Vol.5, p. e13788, 2010.
- [19] F. Takens, "Detecting strange attractors in turbulence Dynamical Systems and Turbulence," Warwick 1980, D. Rand and L.-S. Young (Eds.), Springer Berlin/Heidelberg, Vol.898, pp. 366-381, 1981.
- [20] H. N. Gabow, "An Efficient Implementation of Edmonds Algorithm for Maximum Matching," *JACM*, Vol.23, No.2, pp. 221-234, 1976.
- [21] P. Tichavsky and Z. Koldovsky, "Optimal pairing of signal components separated by blind techniques," *IEEE Signal Processing Letters*, Vol.11, No.2, pp. 119-122, 2004.
- [22] A. Dapena, M. F. Bugallo, and L. Castedo, "Separation of convolutive mixtures of temporally-white signals: a novel frequency-domain approach," In: *Proc. Int. Conf. Independent Component Analysis and Blind Source Separation (ICA)*, San Diego, USA, pp. 315-320, 2001.

**Name:**

Guohun Zhu

**Affiliation:**

Associate Professor, School of Electronic Engineer and Automatic, Guilin University of Electronic Technology

**Address:**

No.1, Jinji Road, Guilin 541004, China

**Brief Biographical History:**2006- Associate Professor, Guilin Institute of Electronic Technology  
2011- University of Southern Queensland**Main Works:**

- computer and network security, biomedical engineering, EDA, graph theory

**Name:**

Yan Li

**Affiliation:**

Department of Mathematics and Computing, Faculty of Sciences, University of Southern Queensland

**Address:**

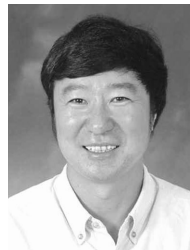
USQ Toowoomba Campus, West Street, Toowoomba, QLD 4350, Australia

**Brief Biographical History:**2007-2008 Senior Lecturer, Department of Mathematics and Computing, University of Southern Queensland  
2009- Associate Professor, Department of Mathematics and Computing, University of Southern Queensland**Main Works:**

- artificial intelligent, neural networks, computer communications and internet technologies, blind signal separation, signal/image processing technologies and their applications on medical bioinformatics

**Membership in Academic Societies:**

- The Institute of Electrical and Electronics Engineers (IEEE)
- Association for Computing Machinery (ACM)

**Name:**

Peng (Paul) Wen

**Affiliation:**

Associate Professor, Faculty of Engineering and Surveying, University of Southern Queensland

**Address:**

USQ Toowoomba Campus, West Street, Toowoomba, QLD 4350, Australia

**Main Works:**

- biomedical engineering, control system and signal processing

**Membership in Academic Societies:**

- The Institute of Electrical and Electronics Engineers (IEEE)